Supplementary Materials

Synergistic internal-external disorder to activate electrochemically inert maricite $NaFePO_4$

Wei Hu[1], Sen Dong[1], Yue Zhang[1,*], Bin Tang[2,*], Yifan Wu[3], Yakun Tang[1,*], Jinlin Li[4], Lang Liu[1], Zhen Zhou[2,4]

[1]Key Laboratory of Energy Materials Chemistry, Ministry of Education, College of Chemistry, Xinjiang University, Urumqi 830017, Xinjiang, China.
[2]Interdisciplinary Research Center for Sustainable Energy Science and Engineering (IRC4SE2), School of Chemical Engineering, Zhengzhou University, Zhengzhou 450001, Henan, China.

[3]Future Battery Research Center, Global Institute of Future Technology, Shanghai Jiao Tong University, Shanghai 200240, China.
[4]Institute of New Energy Material Chemistry, Renewable Energy Conversion and Storage Center (ReCast), School of Materials Science and Engineering, Nankai University, Tianjin 300350, China.

***Correspondence to:** Prof. Yue Zhang, Prof. Yakun Tang, Key Laboratory of Energy Materials Chemistry, Ministry of Education, College of Chemistry, Xinjiang University, Urumqi 830017, Xinjiang, China. E-mail: yuezhang@xju.edu.cn; yktang@xju.edu.cn; Dr. Bin Tang, Interdisciplinary Research Center for Sustainable Energy Science and Engineering (IRC4SE2), School of Chemical Engineering, Zhengzhou University, Zhengzhou 450001, Henan, China. E-mail: tangbin@zzu.edu.cn

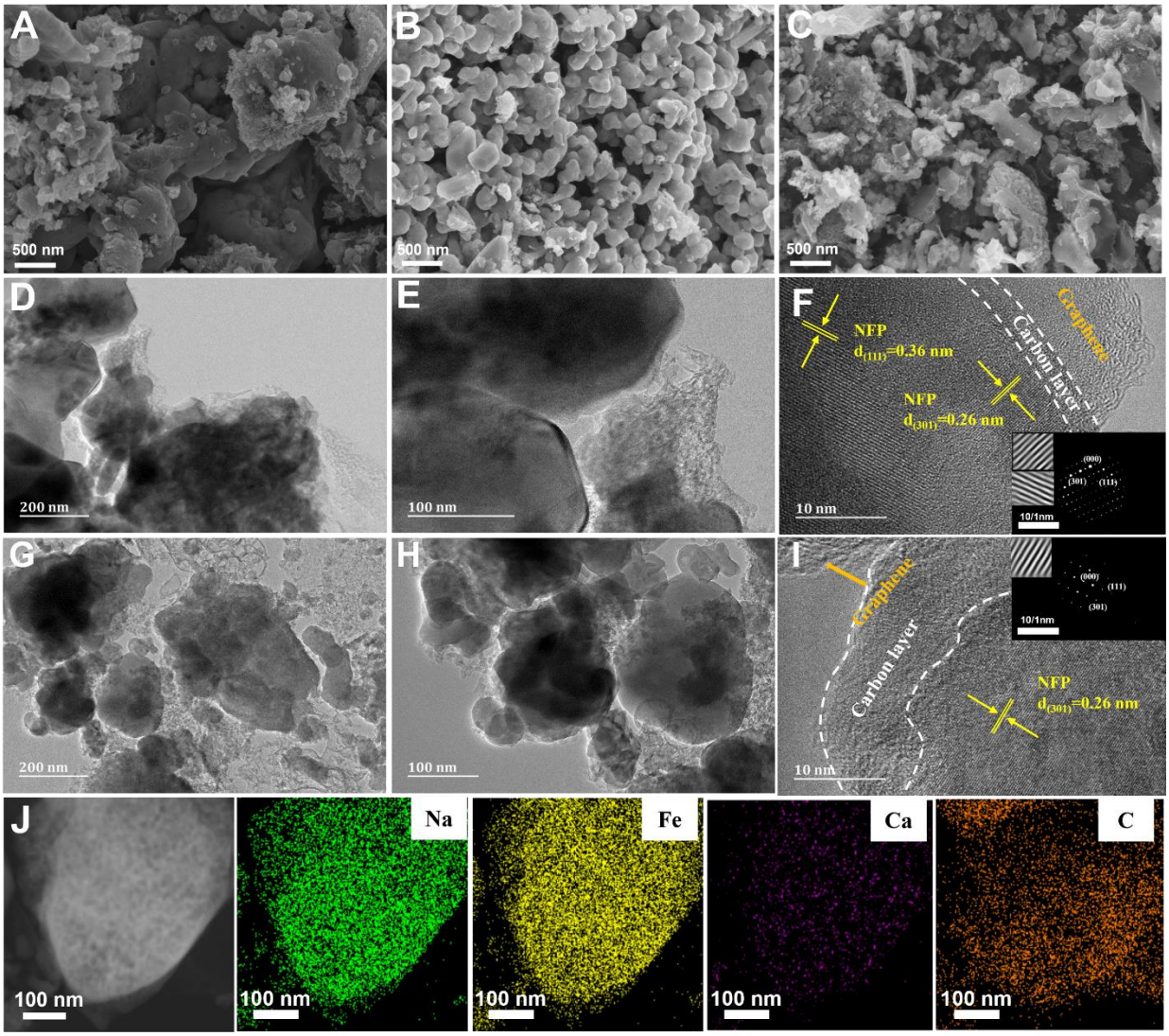

Figure S1. SEM images of NFP/C (A), NFP/C-H (B) and NFP/C-$T_{0.01}$ (C) to NFP/C-$T_{0.01}$ (B), NFP/C-H (C); (D-F) TEM and HRTEM images of NFP/C-$T_{0.01}$; (G-I) TEM and HRTEM images of NFP/C-H; (J) EDS images of NFP/C-$T_{0.01}$.

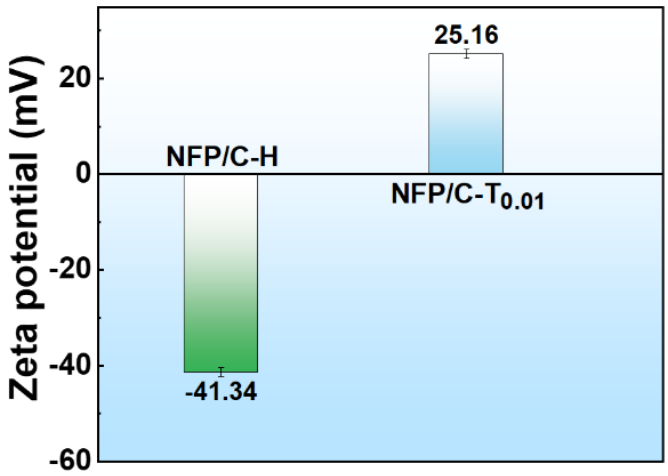

Figure S2. Zeta potential values of the NFP/C, NFP/C-H and NFP/C-$T_{0.01}$ samples powder dispersed in H_2O.

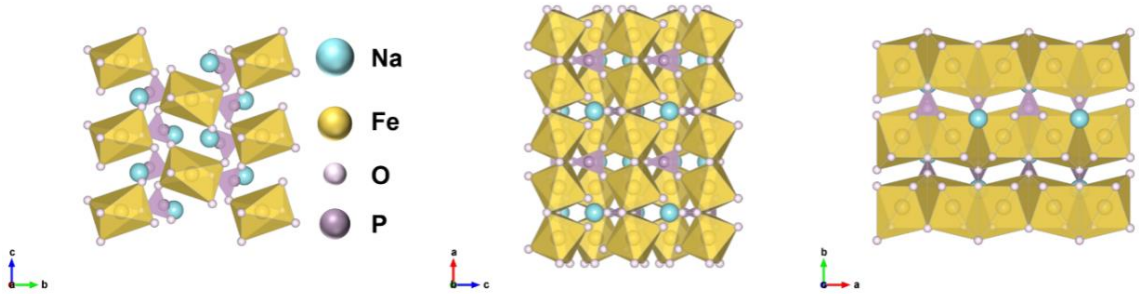

Figure S3. Crystal structure schematics of NFP along different orientations.

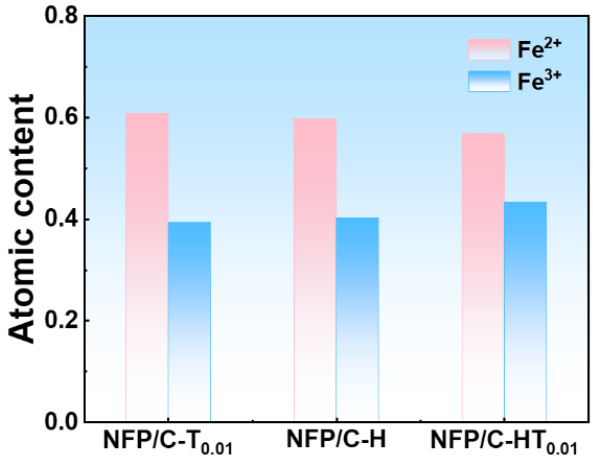

Figure S4. Ratio of Fe^{2+} to Fe^{3+} in NFP/C- $T_{0.01}$, NFP/C-H, and NFP/C-$HT_{0.01}$.

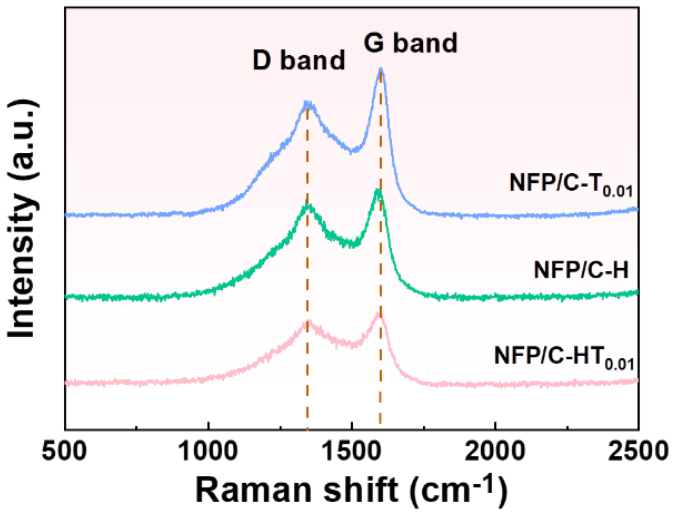

Figure S5. Raman spectra of NFP/C- $T_{0.01}$, NFP/C-H and NFP/C-$HT_{0.01}$ samples.

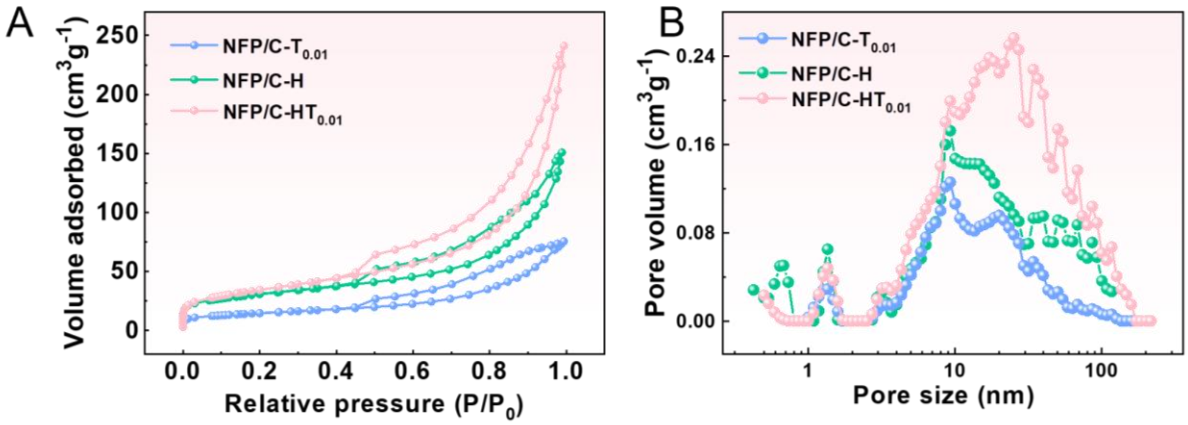

Figure S6. (A) N_2 adsorption-desorption isotherm and (B) pore size distribution curve of NFP/C-H, NFP/C-$T_{0.01}$ and NFP/C-$HT_{0.01}$ samples.

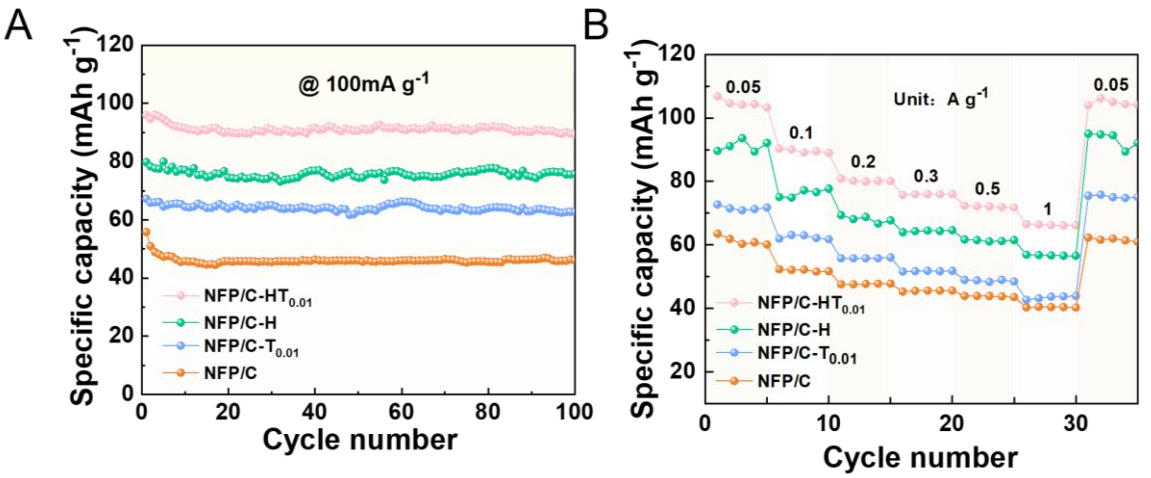

Figure S7. (A) Cycle performance at a current density of 100 mA g^{-1} and (B) rate performance of NFP/C, NFP/C-H, NFP/C-$T_{0.01}$ and NFP/C-$HT_{0.01}$ samples.

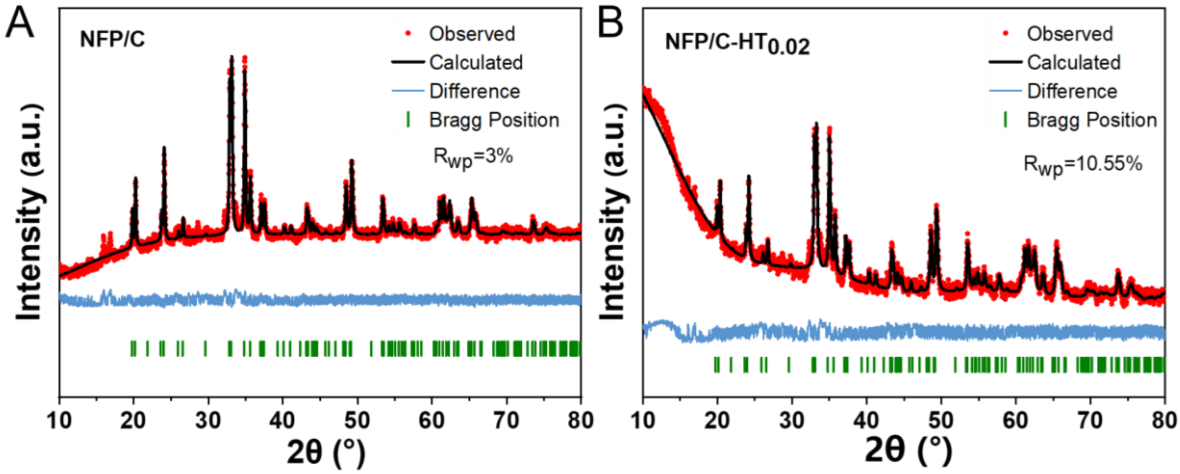

Figure S8. Rietveld refinements of NFP/C (A) and NFP/C-$HT_{0.02}$ (B).

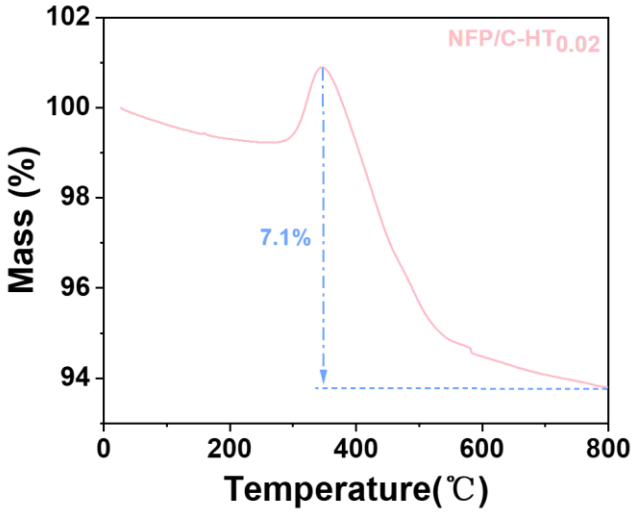

Figure S9. TGA of NFP/C-$HT_{0.02}$ in air atmosphere.

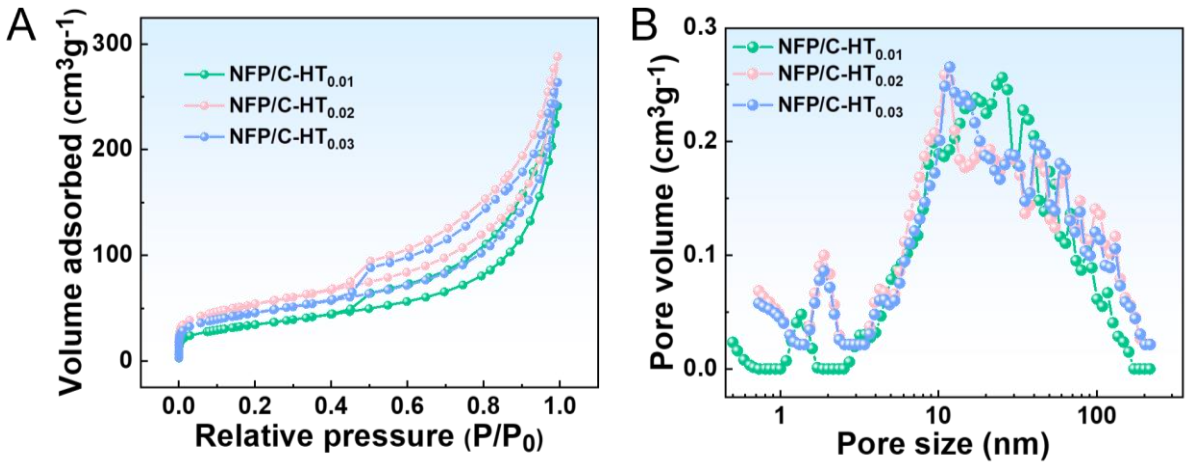

Figure S10. (A) N_2 adsorption-desorption isotherm and (B) pore size distribution curve of NFP/C-$HT_{0.01}$, NFP/C-$HT_{0.02}$ and NFP/C-$HT_{0.03}$ samples.

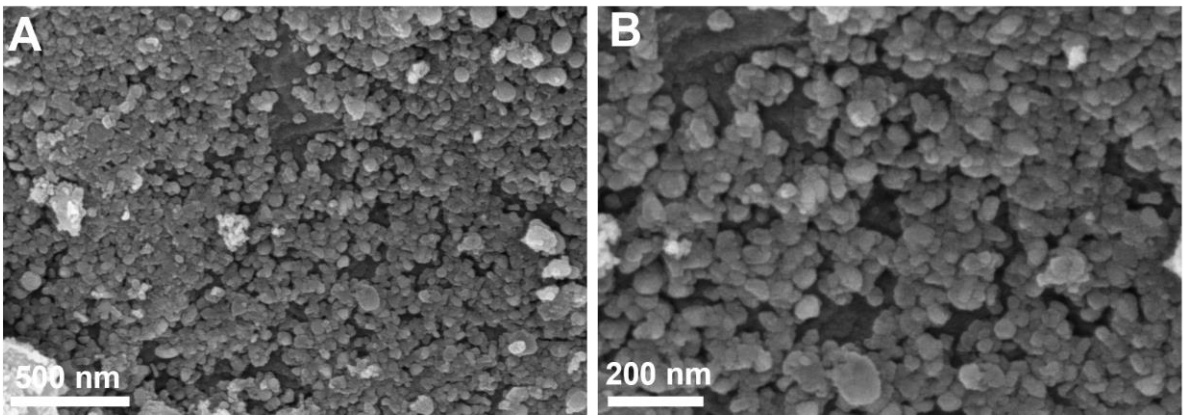

Figure S11. (A, B) SEM images of NFP/C-$HT_{0.03}$.

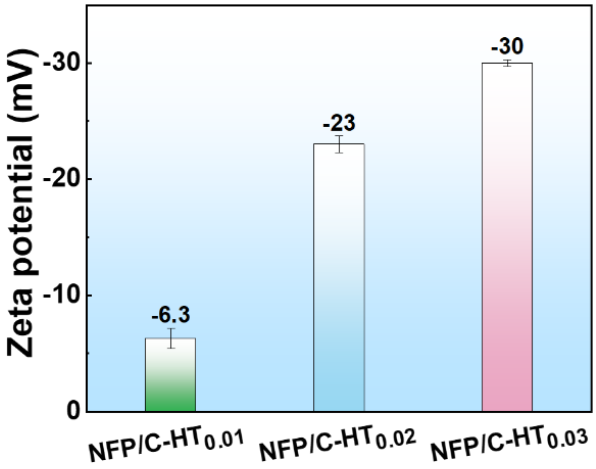

Figure S12. Zeta potential values of the NFP/C-$HT_{0.01}$, NFP/C-$HT_{0.02}$ and NFP/C-$HT_{0.03}$ samples powder dispersed in H_2O.

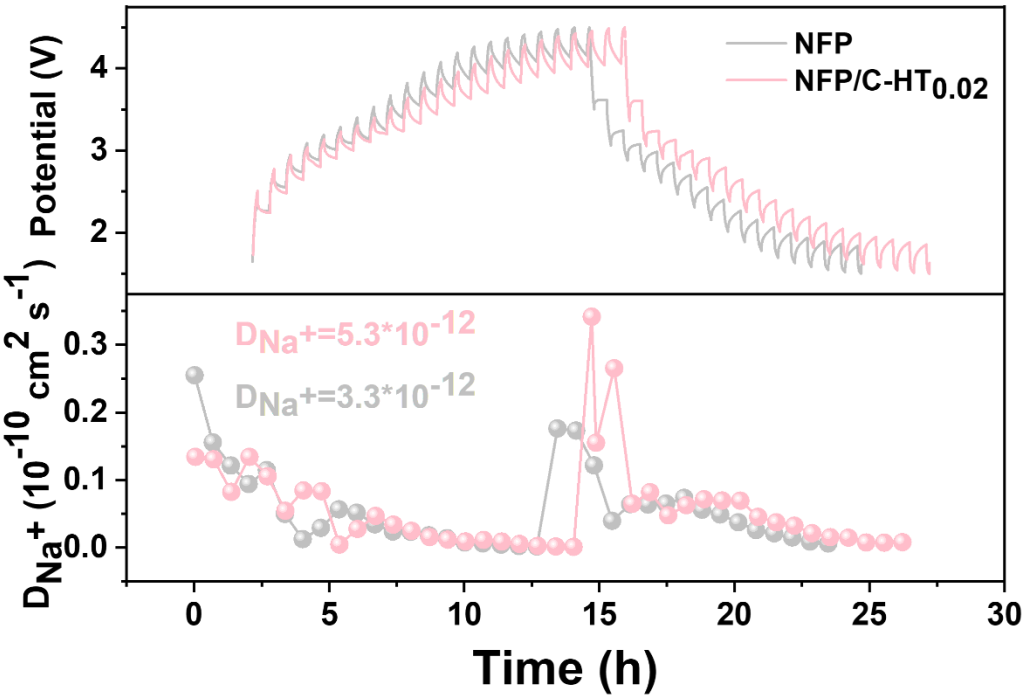

Figure S13. GITT curves and Na^+ diffusion coefficients of NFP/C-$HT_{0.02}$ and NFP.

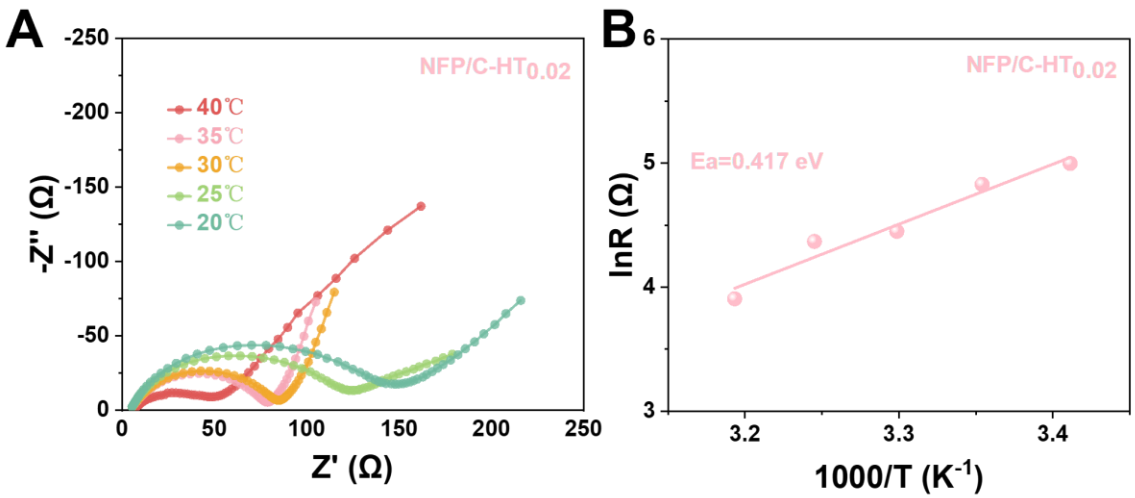

Figure S14. Nyquist plots of NFP/C-$HT_{0.02}$ at different temperatures (A), and the temperature dependence of the corresponding resistances (B).

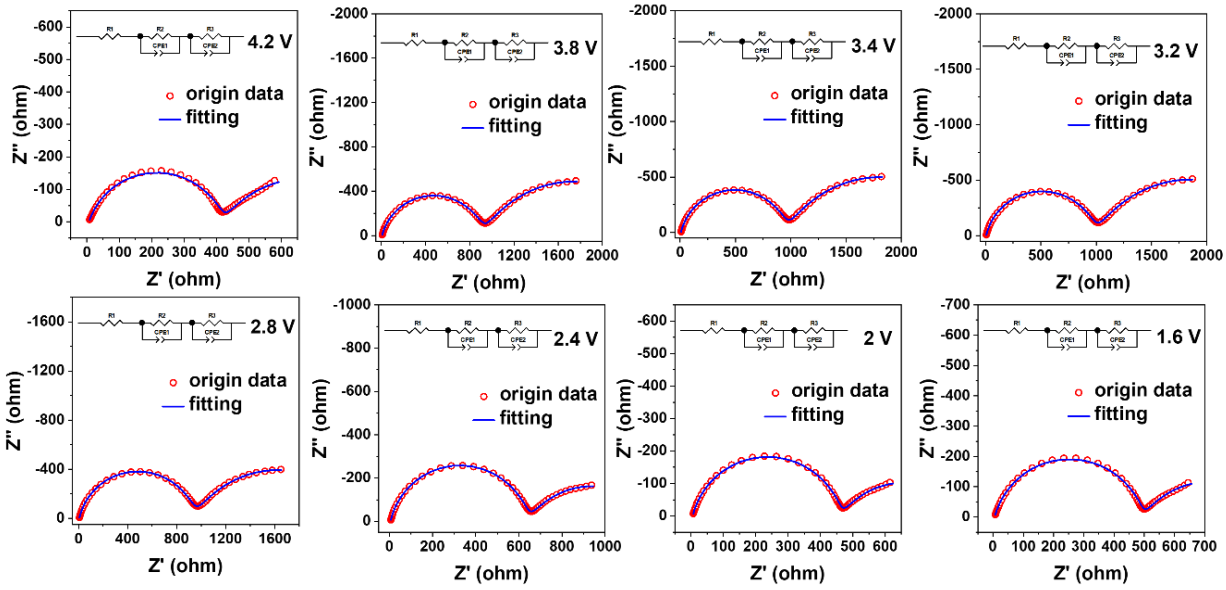

Figure S15. EIS of NFP/C-HT$_{0.02}$ at Various Discharge Voltages.

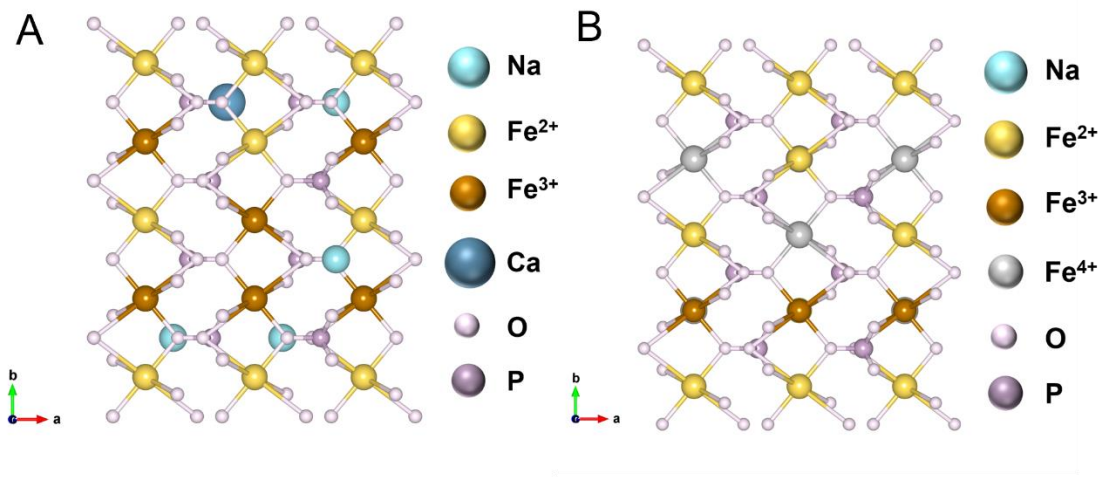

Figure S16. Crystal structure schematic of NFP featuring Fe^{3+} (A) and Fe^{4+} (B).